

## High-Temperature Molecular Magnets Based on Cyanovanadate Building Blocks: Spontaneous Magnetization at 230 K

William R. Entley and Gregory S. Girolami\*

The molecule-based magnetic materials  $\text{Cs}_2\text{Mn}^{\text{II}}[\text{V}^{\text{II}}(\text{CN})_6]$  (1) and  $(\text{Et}_4\text{N})_{0.5}\text{Mn}_{1.25}^{\text{II}}[\text{V}(\text{CN})_5] \cdot 2\text{H}_2\text{O}$  (2) (where Et is ethyl) were prepared by the addition of manganese(II) triflate to aqueous solutions of the hexacyanovanadate(II) ion at 0°C. Whereas 1 crystallizes in a face-centered cubic lattice, 2 crystallizes in a noncubic space group. The cesium salt (1) has features characteristic of a three-dimensional ferrimagnet with a Néel transition at 125 kelvin. The tetraethylammonium salt (2) also behaves as a three-dimensional ferrimagnet with a Néel temperature of 230 kelvin; only two other molecular magnets have higher magnetic ordering temperatures. Saturation magnetization measurements indicate that in both compounds the  $\text{V}^{\text{II}}$  and high-spin  $\text{Mn}^{\text{II}}$  centers are antiferromagnetically coupled. Both 1 and 2 exhibit hysteresis loops characteristic of soft magnets below their magnetic phase-transition temperatures. The high magnetic ordering temperatures of these cyano-bridged solids confirm that the incorporation of early transition elements into the lattice promotes stronger magnetic coupling by enhancing the backbonding into the cyanide  $p^*$  orbitals.

In the last few years, there has been considerable interest in the preparation and properties of “molecular magnets” (1–3). Although a wide variety of such materials

School of Chemical Sciences and Frederick Seitz Materials Research Laboratory, University of Illinois at Urbana-Champaign, 505 South Mathews Avenue, Urbana, IL 61801, USA.

\*To whom correspondence should be addressed.

is now known, most exhibit long-range cooperative magnetic behavior only when they are cooled to rather low temperatures, often well below 30 K (4–12). For example, the one-dimensional (1D) materials  $[\text{Mn}(\text{C}_5\text{Me}_5)_2]$  (TCNE) (Me = methyl) (7),  $[\text{Mn}(\text{F}_3\text{benz})_2]_2(\text{nitMe})$  (10), and  $\text{MnCu}(\text{pbaOH}) \cdot 2\text{H}_2\text{O}$  (6) have magnetic ordering temperatures  $T_N$  of 8.8, 24, and

30 K, respectively (13). In most cases, these low values are consequences of the low dimensionalities of the lattices: magnetic interactions between 1D chains are weak because they must propagate through space rather than through bonds (14, 15). Recently, however, Miller and co-workers have reported an amorphous solid of approximate stoichiometry  $V(\text{TCNE})_2 \cdot \frac{1}{2}\text{CH}_2\text{Cl}_2$ , which is the first example of a molecular material that is magnetic at room temperature (16). The high magnetic ordering temperature  $T_N$  of this solid undoubtedly reflects the presence of strong 3D interactions among the adjacent spin centers (15, 16). Unfortunately, the discovery of  $V(\text{TCNE})_2 \cdot \frac{1}{2}\text{CH}_2\text{Cl}_2$  has not yet led to the development of a general route to molecular magnets with high  $T_N$ .

One potential general route to the synthesis of molecular magnets with  $T_N$  above 300 K is to make analogs of Prussian blue. Prussian blue is a mixed-valent cyanoferrate of stoichiometry  $\text{Fe}^{\text{III}}_4[\text{Fe}^{\text{II}}(\text{CN})_6]_3 \cdot x\text{H}_2\text{O}$  in which iron(II) and iron(III) centers form a cubic lattice linked by cyanide ligands. Prussian blue has a rather low magnetic ordering temperature of 5.6 K: The paramagnetic  $\text{Fe}^{3+}$  ions are weakly interacting because they are separated by intervening diamagnetic  $\text{Fe}^{2+}$  centers (17). In contrast, analogs of Prussian blue in which all of the centers are paramagnetic are especially attractive as candidates for new molecular magnets for several reasons: (i) the linear  $M\text{--}CN\text{--}M'$  bridges promote the formation of strong magnetic interactions between adjacent spin centers, (ii) the solids can be easily prepared at room temperature from well-characterized cyanometallate building blocks, and (iii) a wide range of metals with different spin states and oxidation states can be substituted into the lattice (18, 19). These features allow consider-

able control over the nature and the magnitude of the local magnetic exchange interactions.

The magnetic properties of a number of Prussian blue analogs have been described (18, 20–23), and the nature of the exchange interactions has been discussed (24); the antiferromagnetic interactions, which are thought to propagate principally through the empty  $\pi^*$  orbitals of the cyanide ligand, are generally dominant (18, 20, 21). Because  $T_N$  is directly related to the magnitude of the spin coupling between adjacent metal centers (25), it should be possible to increase  $T_N$  in Prussian blue analogs by increasing the extent of  $\pi$ -back-bonding into the cyanide  $\pi^*$  orbitals. One way to accomplish this is to substitute into the structure metals that have high-energy  $t_{2g}$  orbitals. In particular, it might be possible to prepare solids with  $T_N$  near 300 K by substituting low-valent V or Ti centers into a cyanide-bridged 3D lattice, but to our knowledge no such materials have been reported. We describe herein the synthesis, characterization, and magnetic properties of V-containing analogs of Prussian blue; one of these solids exhibits spontaneous magnetization at 230 K. The cyanovanadate reagents we have used as molecular building blocks are the potassium and tetraethylammonium salts of the hexacyanovanadate(II) ion:  $\text{K}_4[\text{V}(\text{CN})_6]$  (26) and  $(\text{NEt}_4)_4[\text{V}(\text{CN})_6]$  (Et = ethyl) (27).

Addition of  $\text{Mn}(\text{OSO}_2\text{CF}_3)_2(\text{CH}_3\text{CN})_2$  (28) to an aqueous solution of  $\text{CsOSO}_2\text{CF}_3$  (28) and  $\text{K}_4[\text{V}(\text{CN})_6]$  under argon at 0°C yields an air-sensitive green solid (29) of stoichiometry  $\text{Cs}_2\text{Mn}^{\text{II}}[\text{V}^{\text{II}}(\text{CN})_6]$  (**1**) (Fig. 1). The infrared (IR) spectrum of this material shows a strong  $\nu_{\text{CN}}$  stretch at 2097  $\text{cm}^{-1}$  and a shoulder at 2062  $\text{cm}^{-1}$ . The frequency of the former band is consistent with the presence of bridging cyanide groups that are C-bound to  $\text{V}^{\text{II}}$  and N-bound to  $\text{Mn}^{\text{II}}$  (19). The shoulder at 2062  $\text{cm}^{-1}$  suggests that there is some disorder in the cyanide positions (18, 22, 30); for ex-

ample, some of the bridging cyanide ligands are C-bound to  $\text{Mn}^{\text{II}}$  and N-bound to  $\text{V}^{\text{II}}$ . The powder x-ray diffraction (XRD) pattern of **1** is able to be indexed to a face-centered-cubic (fcc) lattice with  $a = 10.66 \text{ \AA}$ ; no extraneous peaks are present in the XRD pattern. This information and the magnetic studies below show that the lattice of **1** consists principally of alternating  $\text{V}^{\text{II}}$  ( $t_{2g}^3$ ) and  $\text{Mn}^{\text{II}}$  ( $t_{2g}^3e_g^2$ ) centers bridged by cyanide ligands; the  $\text{Cs}^+$  cations occupy the cube “interiors” described by the cyanide-bridged lattice. The near-IR spectrum shows no intervalence transfer band, which indicates that electron transfer between the  $\text{V}^{\text{II}}$  and  $\text{Mn}^{\text{II}}$  centers is not occurring.

The room-temperature value of  $\chi T$  is 6.2(3)  $\text{cm}^3 \text{ K mol}^{-1}$  (where  $\chi$  is the magnetic susceptibility and  $T$  is the temperature; numbers in parentheses are standard errors in the last digit); this value closely agrees with the value of 6.3  $\text{cm}^3 \text{ K mol}^{-1}$  calculated for a thermally random mixture of equal populations of  $S = 5/2$  and  $S = 3/2$  spin centers. As the sample is cooled,  $\chi T$  gradually decreases and reaches a minimum near 200 K (Fig. 2, inset); a fit of the data to the Curie-Weiss equation  $\chi = C/(T - \theta)$  (where  $C$  is a constant) over the temperature range from 290 to 265 K yields a Weiss constant,  $\theta$ , of  $-250 \text{ K}$ . The minimum in the curve of  $\chi T$  versus  $T$  (4) and the negative Weiss constant indicate that the adjacent spin centers in **1** are antiferromagnetically coupled.

At lower temperatures, **1** becomes strongly magnetic, as shown by the rapid increase in the magnetization below 125 K (Fig. 2). Fitting the high-temperature reciprocal susceptibility of **1** to a hyperbola based on Néel's theory (31) confirms that  $T_N$  is 125 K. We established the antiferromagnetic nature of the interaction between the adjacent  $\text{V}^{\text{II}}$  and  $\text{Mn}^{\text{II}}$  centers quantitatively by measuring the field dependence of the magnetization of **1** at 4.5 K (Fig. 3). The saturation magnetization at 70 kG is  $1.34(6) \times 10^4 \text{ G cm}^3 \text{ mol}^{-1}$ ; this value is consistent with the calculated

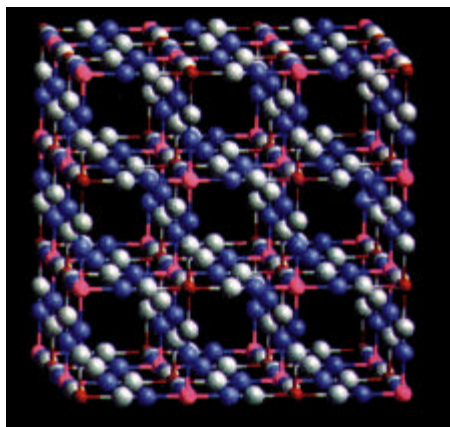


Fig. 1. Structure of  $\text{Cs}_2\text{Mn}^{\text{II}}[\text{V}^{\text{II}}(\text{CN})_6]$  (**1**). Each cube interior is occupied by a  $\text{Cs}^+$  ion. The maroon spheres represent  $\text{V}^{\text{II}}$  centers ( $\text{C}_6$  coordination environments), and the pink spheres represent  $\text{Mn}^{\text{II}}$  centers ( $\text{N}_6$  coordination environments).

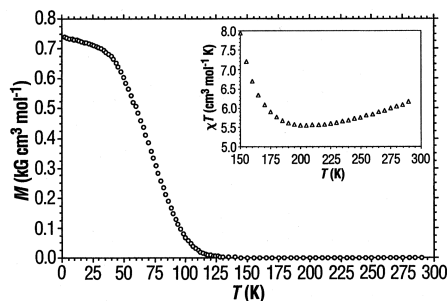


Fig. 2. Temperature dependence of the magnetization  $M$  per formula unit of  $\text{Cs}_2\text{Mn}^{\text{II}}[\text{V}^{\text{II}}(\text{CN})_6]$  (**1**) in an applied magnetic field  $H$  of 25 G. The inset shows the minimum observed at 200 K in a plot of  $\chi T$  versus  $T$ .

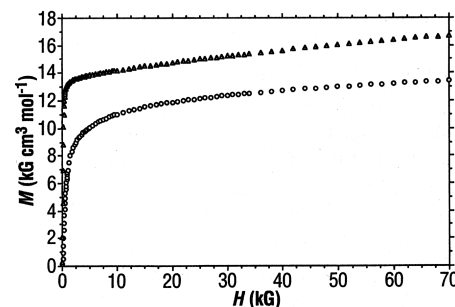


Fig. 3. Field dependence of the magnetization at 4.5 K of  $\text{Cs}_2\text{Mn}^{\text{II}}[\text{V}^{\text{II}}(\text{CN})_6]$  (**1**) (O) and  $(\text{Et}_4\text{N})_{0.5}\text{Mn}_{1.25}[\text{V}(\text{CN})_6] \cdot 2\text{H}_2\text{O}$  (**2**) ( $\Delta$ ).

value of  $1.12 \times 10^4 \text{ G cm}^3 \text{ mol}^{-1}$  expected for equal populations of antiferromagnetically coupled  $\text{V}^{\text{II}}$  and high-spin  $\text{Mn}^{\text{II}}$  centers (32) but inconsistent with the value of  $4.47 \times 10^4 \text{ G cm}^3 \text{ mol}^{-1}$  expected for ferromagnetically coupled centers.

Treatment of  $(\text{NEt}_4)_4[\text{V}(\text{CN})_6]$  with  $\text{Mn}(\text{OSO}_2\text{CF}_3)_2(\text{CH}_3\text{CN})_2$  in the absence of  $\text{Cs}^+$  triflate yields a yellow compound tentatively formulated on the basis of micro-analytical data as  $(\text{Et}_4\text{N})_{0.5}\text{Mn}_{1.25}[\text{V}(\text{CN})_5] \cdot 2\text{H}_2\text{O}$  (**2**) (29); the stoichiometry varies slightly depending on reaction conditions, and the possibility that the solid is a mixture of distinct species cannot be ruled out. Besides bands that are a result of the  $(\text{NEt}_4)^+$  cation, the IR spectrum of **2** contains features attributable to the cyanide groups at 2094 and 2079  $\text{cm}^{-1}$  with a shoulder at 2066  $\text{cm}^{-1}$ , and clearly shows that there are no terminal vanadyl species present. The frequencies of the  $\nu_{\text{CN}}$  stretching bands are characteristic of bridging cyanide ligands (19), but evidently several different cyanide environments are present in **2**. There is no intervalence electron transfer band in the near-IR spectrum.

Unlike the behavior seen for **1**, the curve of  $\chi T$  versus  $T$  for **2** exhibits no minimum as the sample is cooled from 350 K; instead,  $T$  gradually increases as the temperature decreases (Fig. 4, inset). Most interesting, however, is the  $T_N$  value of 230 K (corresponding to the sharp rise in the magnetization as the sample is cooled; see Fig. 4). Among reported molecular magnetic materials, only two exhibit higher  $T_N$  values: the vanadium-TCNE compound of Miller and co-workers (16) ( $T_N$  estimated to be  $\sim 400$  K) and the cyanochromate  $[\text{Cr}_5(\text{CN})_{12}] \cdot 10\text{H}_2\text{O}$  compound of Verdager and co-workers (18) ( $T_N = 240$  K).

The lack of a minimum in the curve of  $\chi T$  versus  $T$  for **2** suggests at first glance that the  $\text{V}^{\text{II}}$  and  $\text{Mn}^{\text{II}}$  spin centers are ferromagnetically coupled, but this conclusion is contradicted by the saturation

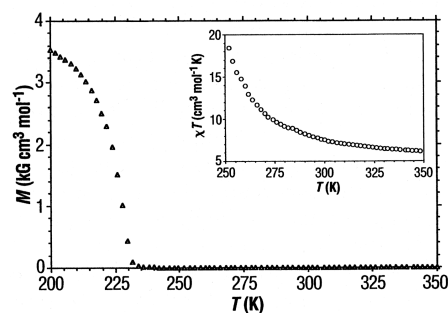


Fig. 4. Temperature dependence of the magnetization  $M$  per formula unit of  $(\text{Et}_4\text{N})_{0.5}\text{Mn}_{1.25}[\text{V}(\text{CN})_5] \cdot 2\text{H}_2\text{O}$  (**2**) in an applied magnetic field  $H$  of 50 G. The inset shows the gradual increase in  $\chi T$  as the sample is cooled below 350 K.

magnetization: The experimental value of  $1.7(1) \times 10^4 \text{ G cm}^3 \text{ mol}^{-1}$  at 4.5 K (Fig. 3) differs significantly from the saturation magnetization of  $5.17 \times 10^4 \text{ G cm}^3 \text{ mol}^{-1}$  calculated by assuming that the metal centers in **2** are ferromagnetically coupled but it agrees closely with the value of  $1.81 \times 10^4 \text{ G cm}^3 \text{ mol}^{-1}$  calculated for antiferromagnetic coupling (32). The lack of a minimum in the curve of  $\chi T$  versus  $T$  for **2** probably means that the minimum lies above the 350 K limit of our data (this being near the temperature at which **2** begins to decompose). In other words, the antiferromagnetic interaction between the  $\text{V}^{\text{II}}$  and  $\text{Mn}^{\text{II}}$  centers is strong enough to depopulate states of high spin multiplicity even at 350 K, and  $\chi T$  continuously increases as the sample is cooled because short-range order keeps the uncompensated moments parallel to each other (9–11). The magnetic data for **2** are thus consistent with bulk ferrimagnetic behavior below its  $T_N$  of 230 K (33, 34).

The powder XRD pattern clearly shows that **2** is polycrystalline but that it does not adopt a fcc structure like **1**. The non-cubic XRD pattern and the unusual ratio of CN to V both suggest that the structure of **2** is more complex than that of **1**; further studies need to be undertaken to determine its 3D structure. Interestingly, Babel has shown that attempts to substitute cations larger than  $\text{Cs}^+$  into the Prussian blue lattice usually give rise instead to lower dimensional structures with substantially decreased magnetic phase-transition temperatures (20). Even though the large  $(\text{NEt}_4)^+$  cations evidently prevent the adoption of the cubic Prussian blue structure, the high value of  $T_N$  suggests that the structure of **2** still consists of a 3D array of interacting spin centers.

Both **1** and **2** exhibit hysteresis below their  $T_N$  values. For **2**, the coercive field is nearly zero at 220 K, although the magnetization as a function of external field strength clearly exhibits an S-shaped

curve characteristic of hysteretic behavior (Fig. 5). As the temperature is lowered, the coercive field of the material increases and reaches a limiting value of  $\sim 24$  G below 50 K. The coercive field for **1** at 10 K is only slightly larger:  $\sim 100$  G (35). The small values of the coercive fields for **1** and **2** lend support to our contention that the metal centers present in these solids are magnetically isotropic  $\text{V}^{\text{II}}$  and high-spin  $\text{Mn}^{\text{II}}$  ions. In contrast, Prussian blue analogs that contain magnetically anisotropic metal centers exhibit considerably larger coercive fields (5, 22).

The V-based Prussian blue analogs that we have prepared confirm our expectation that substitution of early transition metals into the lattice should lead to higher  $T_N$  values. It is especially instructive to compare the behavior of  $\text{Cs}_2\text{Mn}^{\text{II}}[\text{V}^{\text{II}}(\text{CN})_6]$  (**1**) with that of two other isoelectronic and isostructural species,  $\text{CsMn}^{\text{II}}[\text{Cr}^{\text{III}}(\text{CN})_6] \cdot \text{H}_2\text{O}$  (20) and  $\text{Mn}^{\text{II}}[\text{Mn}^{\text{IV}}(\text{CN})_6] \cdot x\text{H}_2\text{O}$  (21). All three compounds have  $d^5$   $\text{Mn}^{\text{II}}$  centers in the weak ligand-field sites ( $N_6$  coordination environments) and  $d^3$  metal centers in the strong ligand-field sites ( $C_6$  coordination environments); the principal difference is that the energies of the  $t_{2g}$  orbitals in the latter sites decrease as the metal changes from  $\text{V}^{\text{II}}$  to  $\text{Cr}^{\text{III}}$  to  $\text{Mn}^{\text{IV}}$ . The relative magnetic ordering temperatures of 125, 90, and 49 K for  $\text{Cs}_2\text{Mn}^{\text{II}}[\text{V}^{\text{II}}(\text{CN})_6]$ ,  $\text{CsMn}^{\text{II}}[\text{Cr}^{\text{III}}(\text{CN})_6] \cdot \text{H}_2\text{O}$ , and  $\text{Mn}^{\text{II}}[\text{Mn}^{\text{IV}}(\text{CN})_6] \cdot x\text{H}_2\text{O}$ , respectively, clearly show that incorporation of transition metals with higher energy  $t_{2g}$  orbitals into the strong ligand-field sites leads to higher magnetic phase-transition temperatures. As the back-bonding with the cyanide  $\pi^*$  orbitals becomes more effective, the coupling between the adjacent spin centers increases. These two V-based molecular magnets represent an important step in the design of molecular magnets with high  $T_N$ . Through judicious choice of cations and metal centers,  $T_N$  values above 300 K should be possible.

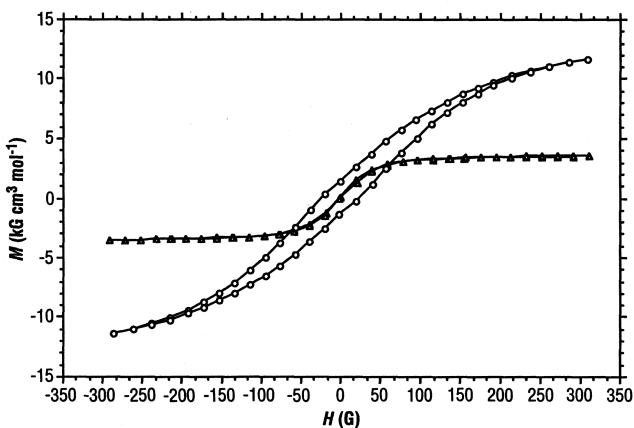


Fig. 5. Hysteresis loops of  $(\text{Et}_4\text{N})_{0.5}\text{Mn}_{1.25}[\text{V}(\text{CN})_5] \cdot 2\text{H}_2\text{O}$  (**2**) at 220 K ( $\Delta$ ) and 50 K ( $\circ$ ).

## REFERENCES AND NOTES

- J. S. Miller and A. J. Epstein, *Angew. Chem. Int. Ed. Engl.* **33**, 385 (1994).
- O. Kahn, *Molecular Magnetism* (VCH, New York, 1993).
- D. Gatteschi, O. Kahn, J. S. Miller, F. Palacio, Eds., *Magnetic Molecular Materials* (Kluwer, Dordrecht, Netherlands, 1991).
- H. O. Stumpf, L. Ouahab, Y. Pei, P. Bergerat, O. Kahn, *J. Am. Chem. Soc.* **116**, 3866 (1994).
- H. O. Stumpf *et al.*, *Chem. Mater.* **6**, 257 (1994).
- K. Nakatani *et al.*, *Inorg. Chem.* **30**, 3977 (1991).
- G. T. Yee *et al.*, *Adv. Mater.* **3**, 309 (1991).
- J. S. Miller *et al.*, *J. Am. Chem. Soc.* **109**, 769 (1987).
- A. Caneschi, D. Gatteschi, A. Lirzin, *J. Mat. Chem.* **4**, 319 (1994).
- A. Caneschi, D. Gatteschi, J. P. Renard, P. Rey, R. Sessoli, *J. Am. Chem. Soc.* **111**, 785 (1989).
- A. Caneschi, D. Gatteschi, P. Rey, R. Sessoli, *Inorg. Chem.* **27**, 1756 (1988).
- P.-M. Allemand *et al.*, *Science* **253**, 301 (1991).
- Abbreviations used are as follows: Me = methyl; TCNE = tetracyanoethylene; F<sub>5</sub>benz = pentafluorobenzoate; nitMe = 2-methyl-4,4,5,5-tetramethyl-4,5-dihydro-1H-imidazolyl-1-oxy-3-oxide; pbaOH = 2-hydroxy-1,3-propanediylbis(oxamate).
- H. O. Stumpf, L. Ouahab, Y. Pei, D. Grandjean, O. Kahn, *Science* **261**, 447 (1993).
- H. O. Stumpf, Y. Pei, O. Kahn, J. Sletten, J. P. Renard, *J. Am. Chem. Soc.* **115**, 6738 (1993).
- J. M. Manriquez, G. T. Yee, R. S. McLean, A. J. Epstein, J. S. Miller, *Science* **252**, 1415 (1991).
- F. Herren, P. Fischer, A. Ludi, W. Hälg, *Inorg. Chem.* **19**, 956 (1980).
- T. Mallah, S. Thiébaud, M. Verdaguer, P. Veillet, *Science* **262**, 1554 (1993).
- A. Ludi and H. U. Güdel, *Struct. Bonding (Berlin)* **14**, 1 (1973).
- D. Babel, *Comments Inorg. Chem.* **5**, 285 (1986).
- R. Klenze, B. Kanellakopulos, G. Trageser, H. H. Eysel, *J. Chem. Phys.* **72**, 5819 (1980).
- W. R. Entley and G. S. Girolami, *Inorg. Chem.* **33**, 5165 (1994).
- R. M. Bozorth, H. J. Williams, D. E. Walsh, *Phys. Rev.* **103**, 572 (1956).
- For a Prussian blue structure, magnetic orbitals on adjacent metal centers M and M' will contribute to the superexchange as follows: e<sub>g</sub>-e<sub>g</sub> and t<sub>2g</sub>-t<sub>2g</sub> combinations (if present) have nonzero overlap and give rise to antiferromagnetic contributions; e<sub>g</sub>-t<sub>2g</sub> combinations (if present) have zero overlap and give rise to ferromagnetic contributions.
- L. Néel, *Ann. Phys. (Paris)* **3**, 137 (1948).
- We prepared K<sub>4</sub>[V(CN)<sub>6</sub>] by adding a solution of KCN (2.56 g, 39.4 mmol) in water (60 ml) to a solution of V(H<sub>2</sub>O)<sub>6</sub>(OSO<sub>2</sub>CF<sub>3</sub>)<sub>2</sub> (36) (1.50 g, 3.28 mmol) in water (25 ml) under argon. The dark brown solution was brought to reflux for 30 min and then was taken to dryness under vacuum. The resulting yellow solid was washed with methanol (30 ml) and extracted into an aqueous 3.5 M KCN solution (70 ml). The orange-yellow extract was filtered, reduced in volume to saturation (~25 ml), and cooled to 5°C to afford orange needles of K<sub>4</sub>[V(CN)<sub>6</sub>]. The yield was 0.66 g (55%).
- We prepared (NEt<sub>4</sub>)<sub>4</sub>[V(CN)<sub>6</sub>] by adding a solution of (NEt<sub>4</sub>)CN (1.37 g, 8.75 mmol) in acetonitrile (30 ml) to a solution of V(H<sub>2</sub>O)<sub>6</sub>(OSO<sub>2</sub>CF<sub>3</sub>)<sub>2</sub> (36) (0.50 g, 1.1 mmol) in acetonitrile (26 ml) under argon. The dark brown solution was brought to reflux for 30 min, filtered, reduced in volume to saturation (~20 ml), and cooled to -20°C to afford a brown solid. The crude product was collected by filtration and dissolved in a solution of (NEt<sub>4</sub>)CN (1.12 g, 72 mmol) in acetonitrile (60 ml). The resulting red-brown solution was brought to reflux for 5 min., filtered, concentrated to ~20 ml, and cooled to -20°C to afford (NEt<sub>4</sub>)<sub>4</sub>[V(CN)<sub>6</sub>] as a brown solid. The yield was 0.17g (21%).
- N. E. Dixon, G. A. Lawrance, P. A. Lay, A. M. Sargeson, H. Taube, *Inorg. Synth.* **24**, 243 (1986).
- Calculated composition for C<sub>6</sub>N<sub>6</sub>Cs<sub>2</sub>MnV (1): C, 13.6%; N, 15.9%; Mn, 10.4%; V, 9.65%. Found: C, 13.7%; N, 16.1%; Mn, 11.6%; V, 10.2%. Calculated composition for C<sub>9</sub>H<sub>13</sub>Mn<sub>1.25</sub>N<sub>5.5</sub>O<sub>2</sub>V (2): C, 30.8%; H, 4.02%; N, 21.99%; Mn, 19.6%; V, 14.5%. Found: C, 30.09%; H, 4.19%; N, 18.2%; Mn, 20.8%; V, 14.8%. Discussions of alternative formulations for 2 such as (Et<sub>4</sub>N)<sub>0.5</sub>Mn<sub>1.25</sub>-[V(CN)<sub>4</sub>(OH)]•H<sub>2</sub>O await additional data.
- E. Reguera, J. F. Bertrán, L. Nuñez, *Polyhedron* **13**, 1619 (1994).
- J. S. Smart, *Am. J. Phys.* **23**, 356 (1955).
- The saturation magnetization was calculated from the formula  $M = g\mu_B N_A S$ , where  $\mu_B$  is the Bohr magneton,  $N_A$  is Avogadro's number, and  $S$  is the net spin per formula unit. The Landé  $g$  factor was assumed to be equal to 2 for both metal centers.
- Further support for a large local antiferromagnetic interaction between the V<sup>II</sup> and Mn<sup>II</sup> spin centers in 2 comes from the  $\chi T$  value of 6.1(2) cm<sup>3</sup> K mol<sup>-1</sup> at 350 K, which is smaller than the value of 7.4 cm<sup>3</sup> K mol<sup>-1</sup> calculated for a thermally random array of Mn<sup>II</sup> ( $S = 5/2$ ) and V<sup>II</sup> ( $S = 3/2$ ) spin centers in a 1.25 to 1 ratio.
- In contrast, the ferrimagnetic Cr-based Prussian blue analogs [Cr<sub>5</sub>(CN)<sub>12</sub>]•10H<sub>2</sub>O and Cs<sub>0.75</sub>[Cr<sub>2.125</sub>(CN)<sub>6</sub>]•5H<sub>2</sub>O, which have  $T_N$  of 240 and 190 K respectively, exhibit minima in their curves  $\chi T$  versus  $T$  below 300 K (18). The absence of such a minimum for 2 suggests that its exchange interactions are stronger than in these cyanochromates.
- The remnant magnetizations for 1 and 2 are ~1.95 × 10<sup>3</sup> G cm<sup>3</sup> mol<sup>-1</sup> at 10 K and ~1.39 × 10<sup>3</sup> G cm<sup>3</sup> mol<sup>-1</sup> at 50 K, respectively.
- D. G. L. Holt, L. F. Larkworthy, D. C. Povey, G. W. Smith, G. J. Leigh, *Inorg. Chim. Acta* **169**, 201 (1990).
- This work was supported by the Department of Energy. The work of W.R.E. was supported by a fellowship from the Department of Chemistry. We thank M. Rosenblatt, D. White, and K. S. Suslick for assistance with Fig. 1.

4 October 1994; accepted 30 December 1994